GEOLOGICAL SURVEY OF CANADA

OPEN FILE 2291

Gravity studies at the Lemieux Dome, Gaspé, Québec

G.W. McNeice
D.E. Boerner
R.D. Kurtz
A.G. Jones

1991

GRAVITY STUDIES AT THE LEMIEUX DOME, GASPÉ, QUÉBEC

by

G. W. McNeice

D. E. Boerner

R. D. Kurtz

A. G. Jones

ABSTRACT

As part of the Federal Gaspé and Lower St. Lawrence Geoscience Program, 83 gravity observations were recorded in August 1988 in the Lemieux Dome region of Gaspé Peninsula, Québec. This survey was designed to aid in the determination of the structure and mineral potential of the first 1000 meters of bedrock. Digital elevation information was used to perform high quality topographic corrections and existing regional gravity observations were used to separate regional and residual components of the gravity field. The new Bouguer anomaly data and contour plots of the Bouguer and residual anomalies are presented in this open file, while the regional data are available from the G.S.C. Geophysical Data Centre.

RÉSUMÉ

Dans le cadre du programme géoscientifique du Plan de dévelopement Gaspésie et Saint-Laurent, 83 stations gravimétriques ont été effectuées en août 1988 dans la région du dôme Lemieux en Gaspésie, Québec. Ce levé fut effectué afin d'aider dans la détermination de la structure du dôme et du potentiel minéral des premiers 1000 m de socle. Des données topographiques numériques furent utilisées pour effectuer des corrections topographiques de haute qualité et les données gravimétriques antérieures ont été utilisées afin de discriminer entre les composantes régionale et résiduelle du champ de gravité. Ce dossier public présente les nouvelles données calculées pour l'anomalie de Bouguer ainsi que la carte de ces mêmes anomalies et celle des anomalies résiduelles. Les données régionales sont disponibles auprès du centre de données géophysiques de la C.G.C..

TABLE OF CONTENTS

1
INTRODUCTION

The Lemieux Dome is a circular region of uplifted Siluro-Devonian sedimentary and volcanic rocks, intruded by multiple generations of small scale sills and stocks. The Dome is situated 45 km south of the St. Lawrence river in north-central Gaspé (figure 1), and has been of some economic interest over the past 80 years, due to the surface exposure of mineralized veins.

Deep drilling of the Lemieux Dome has shown that thermal metamorphism increases with depth. The physiographic structure of the Dome, the existence of mineral zoning in the quartz-carbonate veins cutting the Dome and the presence of porphyry intrusions suggest that the domed structure may have been produced by the upwelling of a large granitic stock. The detailed gravity survey presented in this open file will provide evidence about the nature and composition of the postulated intrusive.

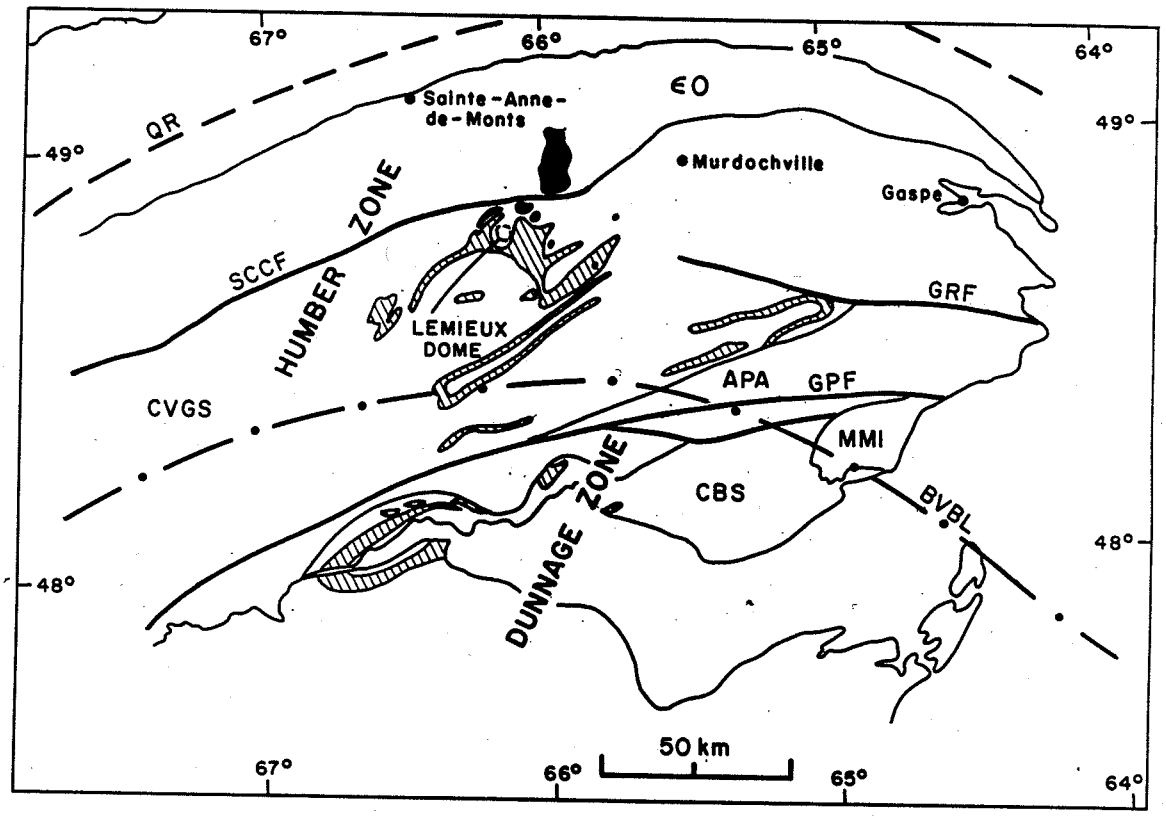

Figure 1 Map of the Gaspé Peninsula showing lithotectonic zones, major faults and location of volcanic and intrusive suites. Lithotectonic zones: ϵO: Cambrian-Ordovician domain; CVGS: Connecticut Valley-Gaspé synclinorium; APA: Aroostook -Percé anticlinorium; CBS: Chaleurs Bay synclinorium; MMI: Maquereau-Mictaw inlier. Faults: SCCF South Chick-Chock fault; GRF: Grande Rivière fault; GPF: Grand Pabos fault. Zone boundaries: BVBL: Baie Verte-Brompton line; QR: Québec Reentrant. Intrusives in black. Volcanic suites denoted by vertical ruling. (after Doyon et al., 1990)

2
REVIEW OF GEOLOGY

The Lemieux Dome is located in north-central Gaspé, Québec, close to the north-western margin of the Appalachian Orogen. Models for the evolution of the Appalachian Orogeny involve the creation and destruction of a late-Precambrian early-Paleozoic proto-Atlantic (Iapetus) ocean as originally suggested by Wilson (1966). The Lemieux Dome rhyolite porphyry intrusives and other sills, dykes, and plugs at Hog's Back, Mont Chauve, Mont Vallières de St. Réal, Mount Brown and Murdochville have been interpreted to be related to the closing stages of the Acadian Orogeny (de Römer, 1974 and Allcock, 1982). Geochemical studies of the Ordovician to Devonian volcanics (Laurent and Bélanger, 1984) and intrusive rocks (Whalen, 1988) suggest an intraplate or post-collisional tectonic setting for these rocks and that the volcanism may be genetically related to tectonic compression and controlled by strike-slip faults. The Lemieux Dome is located just south of the Acadian South Chick-Chock fault (Lebel and Hubert, 1986) in the Connecticut Valley-Gaspé synclinorium (figure 1). The spatial association of the Lemieux Dome intrusives and other intrusives in north-central Gaspé with the South Chick-Chock fault and smaller north trending faults, underlies some of the factors which may have controlled emplacement.

The generalized geology of the Lemieux Dome is shown in figure 2 and figure 3 shows the geology superimposed on a three dimensional topography map. Uplifted Siluro-Devonian sedimentary rocks form a dome structure aproximately 9.5 km in diameter. The sediments of the Dome have been intruded by Devonian gabbros and rhyolite porphyries. These intrusives are orientated primarily in a north-south direction, as are the quartz carbonate veins filling fissures on many parts of the Dome.

A summary of the north-central Gaspé stratigraphy is shown in figure 4.

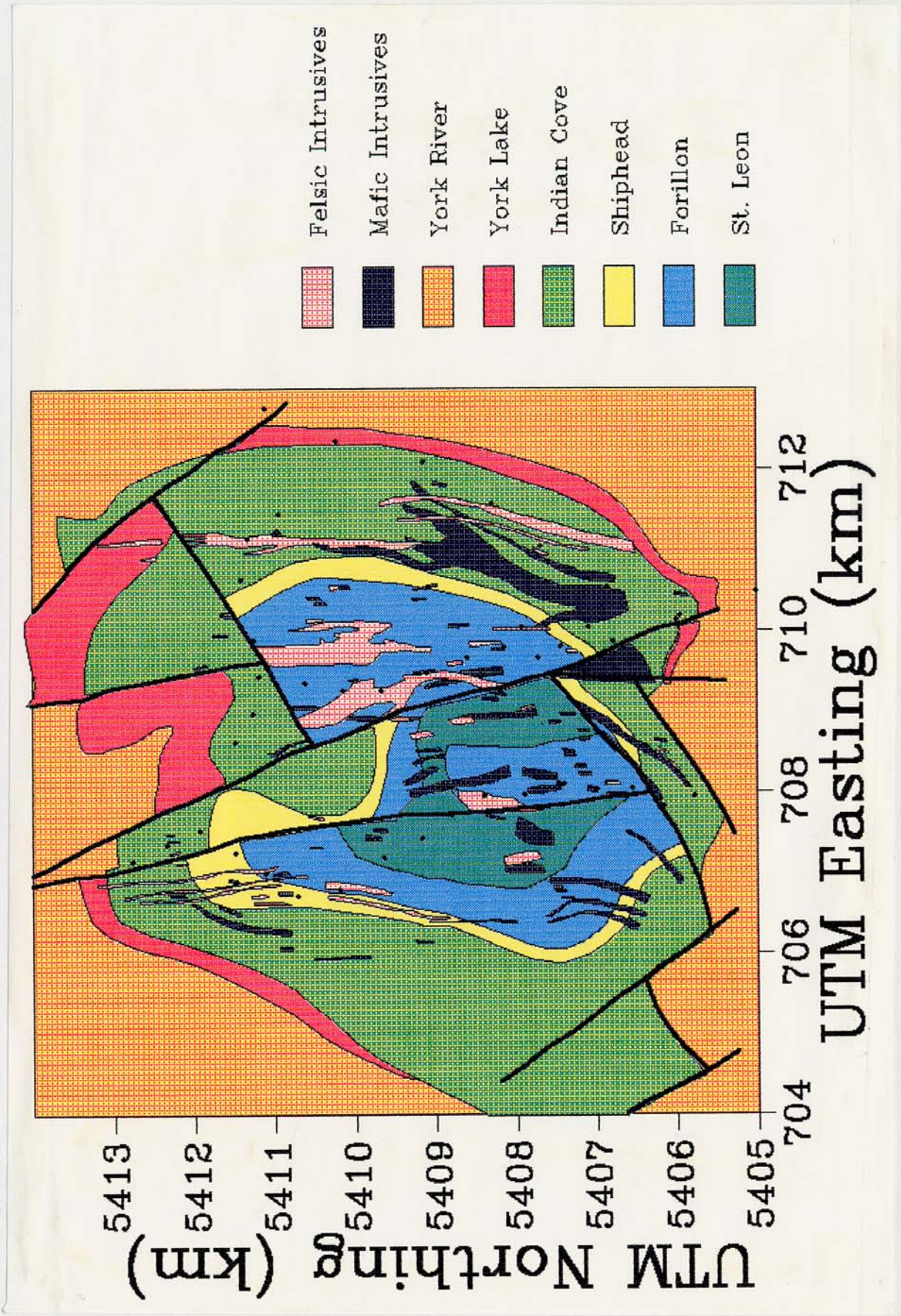

Figure 2 Generalized geology of the Lemieux Dome (formation descriptions in figure 4).

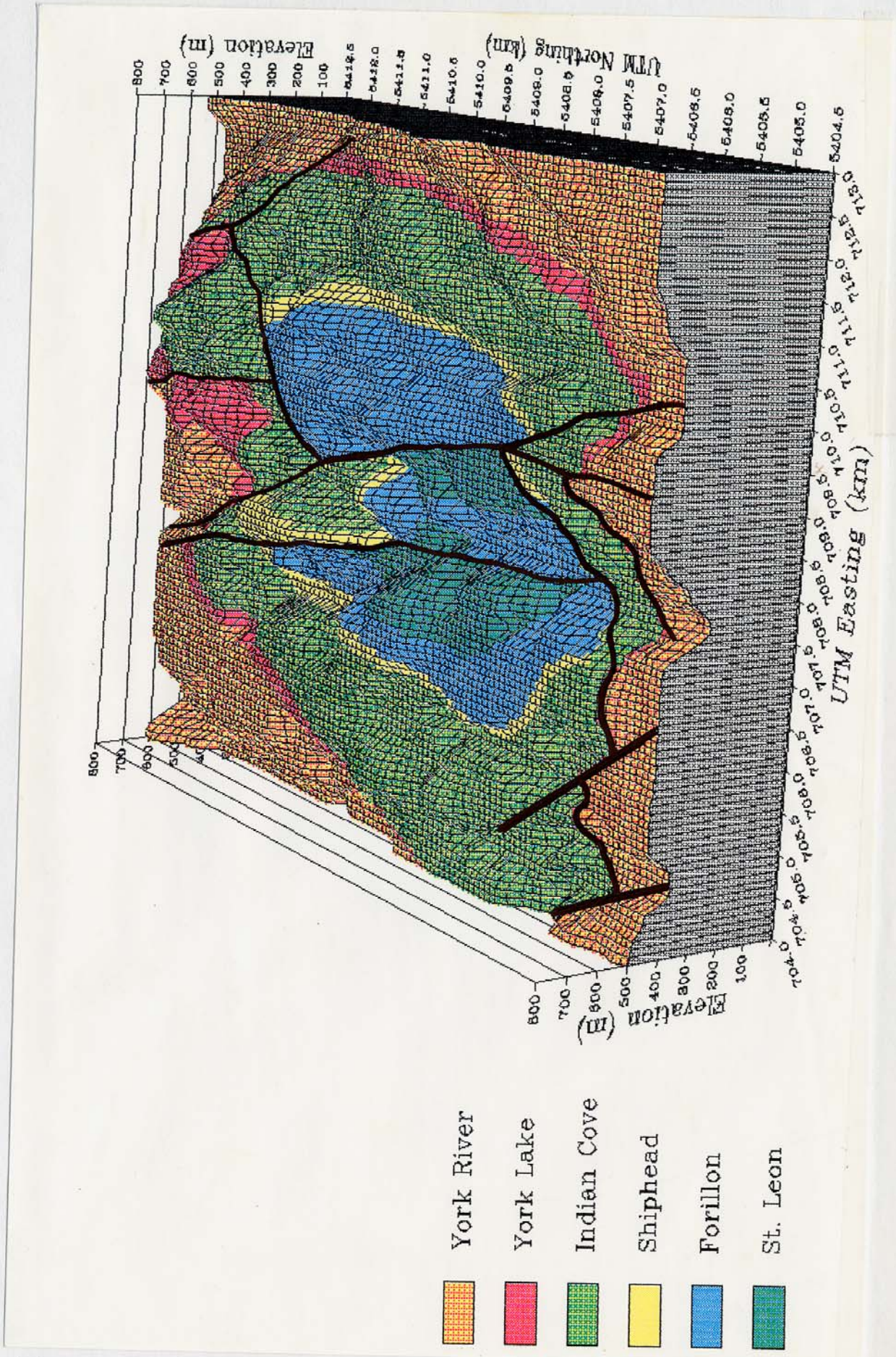

Figure 3 Generalized geology of the Lemieux Dome superimposed on a three dimensional topography map (formation descriptions in Figure 4).

The oldest lithologies exposed at the Lemieux Dome are the upper most beds of the Saint Léon Formation. The upper portion of this formation consists of grey calcareous siltstones or mudstones with red and green mudstone located at the top of the formation. The lower Devonian Gaspé Upper Limestone group overlies the Saint Léon Formation. This group consists of argillaceous to arenaceous limestone, calcareous sandtone to siltstone with minor limestone conglomerate (La Rocque, 1986). The top of this group, the Indian Cove Formation consists of chert and cherty limestone. The Gaspé Sandstone group overlie the Upper Gaspé Limestone group and consists of the interbedded sandstone, mudstone, sandy and cherty limestone of the York Lake Formation, and grey to green arkosic sandstone, siltstone, mudstone and mafic to felsic volcanic rocks of the York River Formation.

Sulphide and oxide mineral-bearing quartz and quartz-carbonate veins occur on many parts of the Dome. These veins are most abundant, largest, and richest in the south central part of the dome. Some of the veins occur at or near intrusion-sedimentary rock contacts, but others are situated up to a kilometer from the nearest intrusive body (Stevens, 1986). The veins range in size and have been observed up to 10 m in width and 800 m in length. Sphalerite, galena, chalcopyrite, pyrite, and hematite are common in the fissure-filling vein material. Mineral occurrences within the veins are vertically and horizontally zoned (horizontal zoning shown in figure 7). The veins contain hematite, pyrite and chalcopyrite in the central part of the dome and sphalerite, galena and dolomite are contained in the veins of the southern portion (Stevens, 1986).

The intrusive rocks of the Lemieux Dome are of two types: gabbros and rhyolite porphyries. The porphyries are generally pink in colour but can also be green, orange, red, beige, or pale blue. Phenocrysts typically make up 10% to 15% of the rock and are set in an aphanitic groundmass. The phenocrysts consist of quartz, plagioclase and potassic feldspar and range in size from 0.5 to 3.0 mm in diameter. The groundmass is composed of quartz and feldspar of

	Group	Nomeclature	Description	Density kg m^{-3}
LOWER DEVONIAN	Gaspé Sandstone	York River Formation	Grey to green arkosic sandstone, mafic to felsic volcanic rocks, ± siltstone and mudstone.	2450 ± 30
		York Lake Formation	Interstratified, grey calcareous sandstone to mudstone with sandy or cherty limestones.	2530 ± 50
	Gaspé Upper Limestone	Indian Cove Formation	Grey sandy or cherty limestone ± calcareous sandstone, siltstone and chert.	2610 ± 30
		Shiphead Formation	Sandy to argillaceous limestone, limestone conglomerate, calcarenite, calcilutite, ± white quartz arenite, calcareous sandstone and mudstone.	2610 ± 30
		Forillon Formation	Argillaceous limestone, black mudstone (predominantly calcareous).	2610 ± 30
UPPER SILURIAN	Chaleurs Group (Gaspé Lower Limestone)	Saint Léon Formation	Calcareous siltstone, Fossiliferous limestone, conglomeratic limestone with interbedded limestone and siltstone, calcareous siltstone with interbedded limestone, red and green shales in upper levels.	2640 ± 50
		Sayabec Formation	Grey, fossiliferous or nodular limestone, sandy limestone at the base.	
		Val Brillant Formation	Basal, white quartz arenite, upper sandy limestone.	
		d'Awantjish Formation	Fossiliferous, dark grey to green shale.	

Figure 4 Summary of the north-central Gaspé stratigraphy (La Rocque 1986).

grain size from 0.1 to 0.2 mm (Stevens, 1986). These porphyry intrusives cut all the formations of the Lemieux Dome and in places cut the gabbroic intrusives. The gabbros are typically melanocratic, fine to coarse-grained equigranular rocks. They are composed of approximately 75% andesine + augite, 15% biotite, and 10% opaque minerals (Stevens, 1986).

Although gabbroic and quartz-felspar porphyry intrusives are common on the Dome, none of them is of sufficient size to have supplied the heat necessary to drive the hydrothermal system responsible for the alteration and vein mineralization. Stevens (1986) concluded that the hydrothermal system was driven by one or more deep seated intrusions, the upper part(s) of which are exposed as quartz-felspar porphyry apophyses, and that vein formation occurred after the emplacement of the apophyses but before they had cooled to the temperature of the host rocks.

3
LEMIEUX DOME GRAVITY SURVEY

In order to understand better the role of intrusives in the formation of the Lemieux Dome, a gravity survey was carried out in August 1988 and consists of observations recorded at a total of 83 locations. Observations at 47 of the sites were recorded at 500 m intervals on two approximately north-south traverses and one east-west traverse (figure 5). The remainder were made at stations spaced 1 km apart along highway 299, which runs north-south just east of the dome. The highway stations stretch from approximately 11 km north of the Dome to 13 km to the south, and were recorded to provide additional information about the regional gravity field.

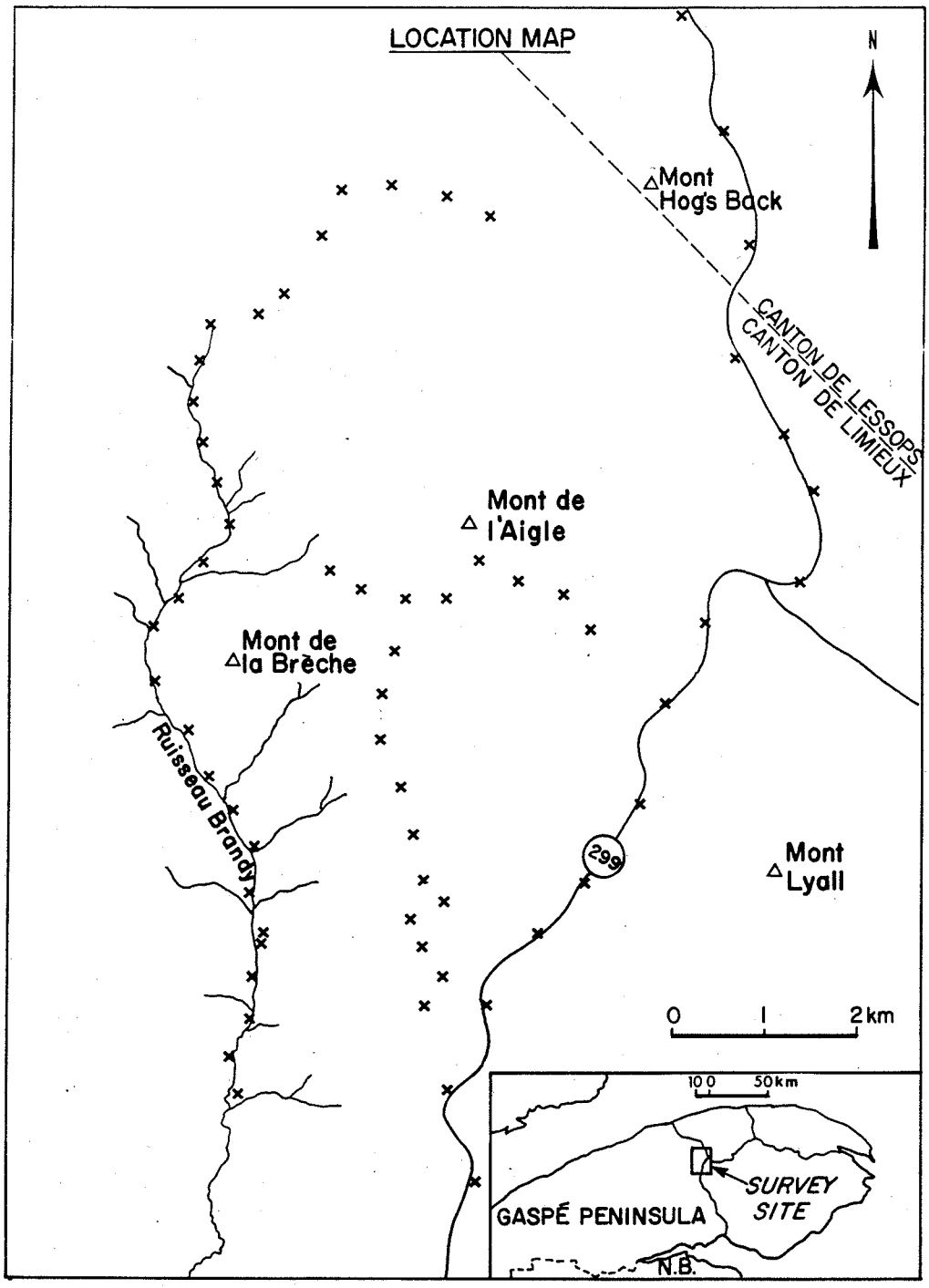

Figure 5 Map of the Lemieux region showing the location of gravity stations. Gravity station locations are indicated by Xs. The locations of only 64 of the stations are depicted in this figure. The remainder of the stations lie to the north and south of the area shown in this figure, along highway 299.

4
SURVEY DATA REDUCTION

The Lemieux Dome gravity observations were made with a La Coste and Romberg gravity meter (no.G278) and the elevation determinations were made with two Wallace and Tiernan altimeters. The observed and processed data are presented in appendix A. Data reduction for the most part was performed with the aid of GSC Gravity Data Centre facilities and is explained in the following paragraphs.

(i) The gravitational effects of tidal variations are typically small, 0.1 mGal or less, and are predictable. The formulae of Longman (1959) were used to calculate corrections for these variations.

(ii) Instrumental drift was estimated from repeated readings at a gravity base station at the beginning and end of each traverse. The drift was assumed to be linear over the time period of the traverse, and the calculated drift rate was then used to correct the observations made during the traverse. Instrument drift averaged 0.014 mGal hour^{-1} over the five traverses.

(iii) The predicted value of gravity at sea-level at any point on the Earth's surface is given by the equation:

$$g_\theta = 978031.85\ [1.0 + 0.005278895\sin^2(\theta) + 0.000023462\sin^4(\theta)]\ \text{mGal},$$

where θ is the latitude of the observation point (based on the 1967 Geodetic Reference System). The latitude of each station was obtained from 1:50,000 maps published by the Surveys and Mapping branch, Department of Energy, Mines and Resources. Station locations are considered to be accurate to ± 50 m, equivalent to an error of ± 0.04 mGal.

(iv) Gravity station elevations were determined on site with two altimeters and corrections were made for variations in air density and barometric pressure drifts. The equations used to perform these corrections are presented in

appendix B. The altimeters were read at a known elevation approximately every hour to permit a linear correction for barometric drift. Elevations determined on the basis of altimeter recordings taken at benchmarks along highway 299 show that these elevations are always accurate to within ± 2 m. Corrections applied to the gravity data, to remove the effects of elevation differences, were performed in three steps.

(a) The Free-Air correction was applied to reduce the gravity observations to a common datum (sea-level). The observed value must be increased by 0.3086 mGal per meter of elevation (Kearey and Brooks, 1984). The ± 2 m error on station elevations leads to an error of ± 0.6 mGal in the free-air corrected gravity values. Second-order corrections, which vary with elevation and latitude, are insignificant with respect to the first order corrections.

(b) The Bouguer correction was performed to remove the effect of the gravitational attraction of the rock between the station and the datum. The gravitational attraction due to this slab is: $\mathrm{BC} = 2\pi\rho\mathcal{G}h$ mGal, where h is the station elevation, $\mathcal{G}$ is the gravitational constant and ρ is the density of the slab (Kearey and Brooks, 1984). Measurements of rock samples from the Gaspé Peninsula made by Tanner and Uffen (1960) indicate an average density of 2630 ± 10 kg m^{-3} (see figure 4), however a density of 2670 kg m^{-3} was used to be consistant with the data in the G.S.C. database and introduces a discrepancy of only 0.8 mGal between the highest and lowest station points.

(c) One further correction was applied to account for the topographic relief in the vicinity of the gravity stations. The terrain corrections were performed by a digital method based on Bible's (1962) terrain correction graticule. To compute the terrain corrections the 250 foot elevation contour lines within a radius of 5 km of each station were digitized on a scale of 1:50,000. Between a radius of 5 km and 22 km of

the stations the 500 foot contour lines were digitized using a 1:250,000 scale topographic map. This digital topographic data, shown in figure 3, were then used to assign relative elevations to each of the 130 compartments of the graticule and the gravitational attraction due to the average **absolute** elevation in each compartment was calculated. The sum of the gravitational contribution of each compartment is the terrain correction for the station on which the graticule is centred. Station locations were selected in the field to minimize terrain contributions from the two innermost zones and they were therefore omitted from the computations. The two innermost zones correspond to a radius of 53 m around the station. The calculated terrain corrections ranged from 2.7 to 14.7 mGal.

Figure 6 is a contour plot of the final Bouguer anomalies and regional data obtained from the GSC Geophysical Data Centre. The Bouguer gravity values probably have an overall error of approximately ± 1 mGal which arises mostly from uncertainty in the station elevations.

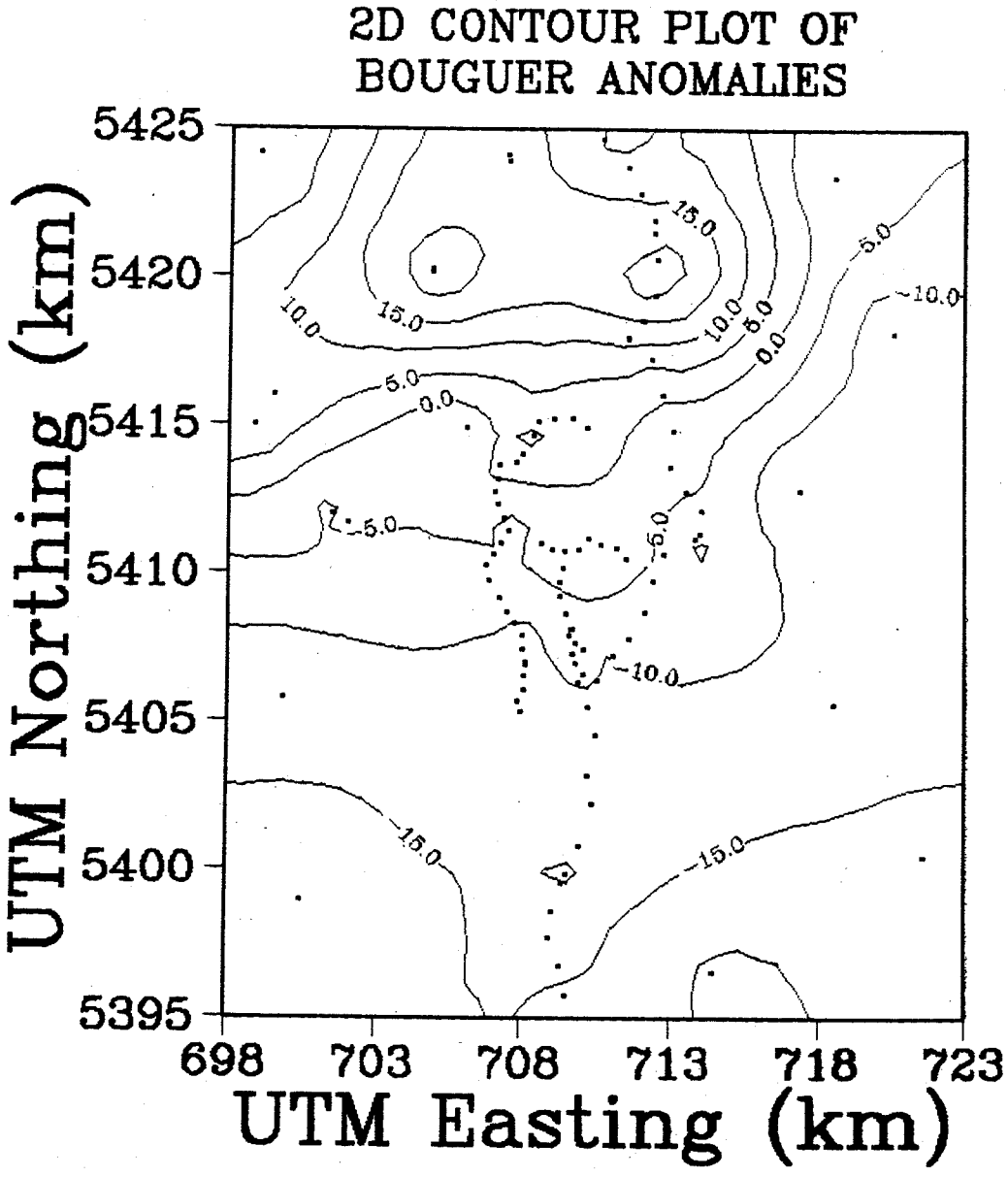

Figure 6 Contour plot of Bouguer anomalies (mGal) in Lemieux Dome region. Gravity stations locations are indicated by dots

5
INTERPRETATION

Before interpreting the gravity observations, the effects of regional gravity trends must be separated from locally produced anomalies. Examination of figure 6 shows that a strong north-south regional gravity trend exists in the survey area. The regional gravity field changes from values of +20 mGal in the north to −20 mGal in the south. This regional gradient is believed to be primarily due to the Mont Albert peridotite body located approximately 8 km to the north of the Lemieux Dome. As there is no unique mass distribution which describes a gravity anomaly, there is no unique way of separating local variations from regional trends on the basis of gravity data alone. Instead one uses the fact that Laplace's equation guarantees the minimum curvature of potential field lines and the curvature diminishes with increasing distance from the source. Thus, small structures cause changes in the observed anomaly on a short spatial scale, while deeper regional structures cause smoother spatial variations. Consequently, the most common method of separating local and regional effects is by spatial filtering.

Unfortunately, the sharp gradient produced by the Mont Albert peridotite body rendered numerical spatial filtering ineffective in this region. Instead a graphical method was employed to separate the residual from the regional field. A contour plot of gravity observations (at approximately 5 km spacing) from the GSC regional gravity data base was used to represent the regional field. This representation of the regional field was subtracted from a similar representation consisting of both the regional data and the new Lemieux Dome data to obtain the local anomaly (figure 7). The consistency of the resulting anomaly pattern is an indication that the separation method was successful.

Examination of the residual anomaly (and original data) clearly indicates the presence of a mass excess, that is, the presence of rock masses having

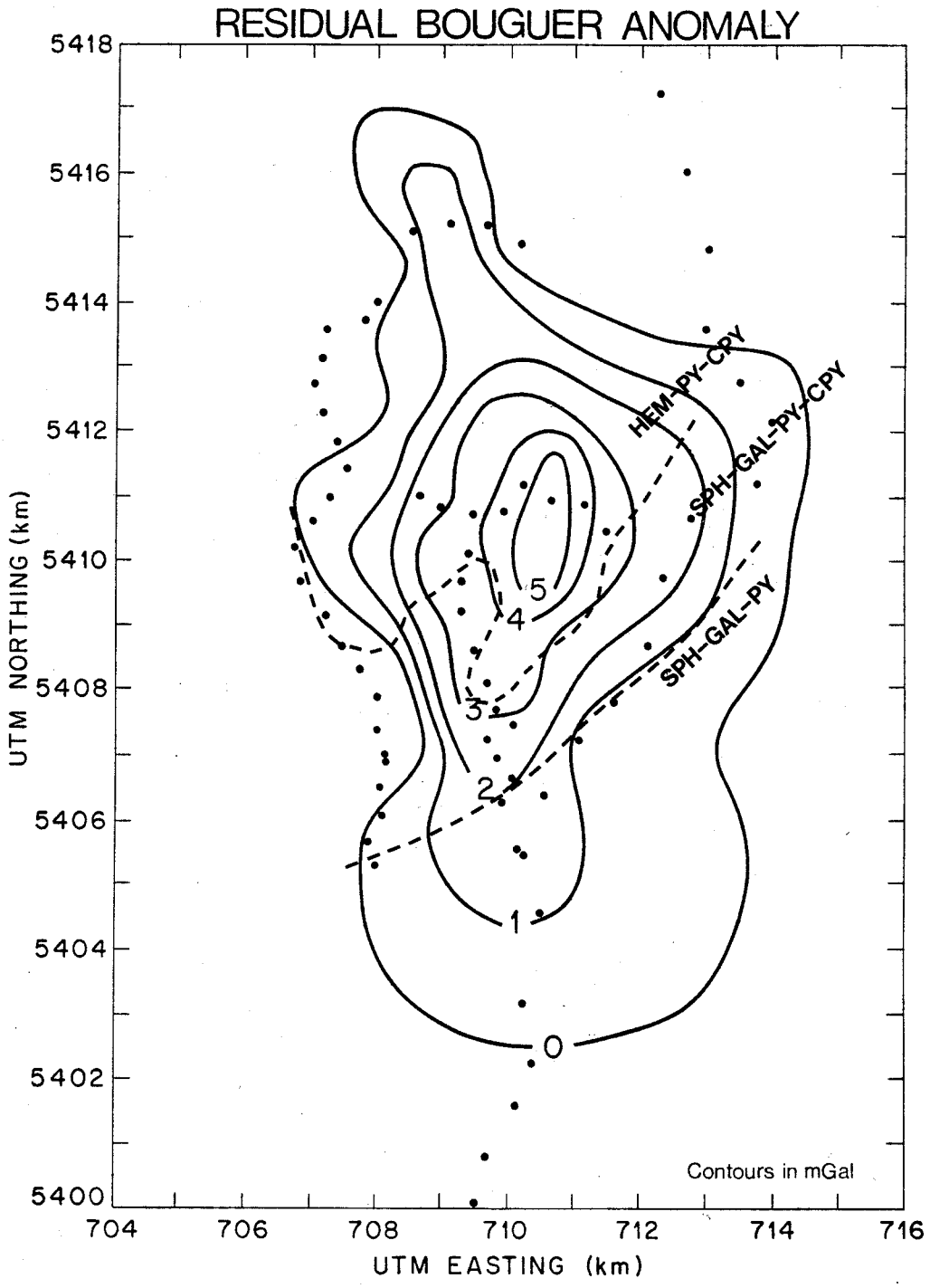

Figure 7 Contour map of the residual Bouguer values (mGal) with horizontal mineral zoning (from Stevens, 1986) superimposed. Gravity station locations are indicated by dots. HEM = hematite, PY = pyrite, CPY = chalcopyrite, SPH = sphalerite, GAL = galena.

densities greater than that of the surrounding rock. The anomaly is definitely elongated in a north-south direction, is almost encircled by the new data, and has a maximum value of 5 mGal in the vicinity of Mont de l'Aigle.

5.1 Estimation of Physical Properties :

Although gravity interpretations are non-unique, the total anomalous mass of the causative body can be uniquely determined from the observed data. Anomalous mass is calculated via an equation derived from Gauss' flux theorem in potential theory involving a surface integration over the area of the anomaly. In this study a numerical approximation to the surface integral was used. The survey area was divided into n grid squares, all of equal area Δa and the average anomaly Δg was found in each grid cell. The total anomalous mass (M_a) is then calculated from

$$M_a = \frac{1}{2\pi\mathcal{G}} \sum_{i=1}^{n} \Delta g_i \Delta a_i = \frac{\Delta a}{2\pi\mathcal{G}} \sum_{i=1}^{n} \Delta g_i \qquad \text{kg,}$$

where $\mathcal{G}$ is the gravitational constant. It is important to emphasize that anomalous mass is the one unique parameter obtainable from gravity interpretation.

Numerical surface integration of the residual gravity anomaly yielded a value of 2.24×10^{12} kg for the excess mass of the body(s) producing the anomaly. Any geological models which represent the actual mass distribution in the Earth must have this anomalous mass. This value may be an underestimate of the true excess mass, since the integration was performed over a finite surface area defined by the extent of the data and not over an infinite horizontal plane as required by theory. As well, the excess mass estimate depends on the subjective local-regional gravity field separation.

Although the observed anomaly appears to be somewhat elongated, the anomaly produced by a simple sphere was found to be a reasonable approximation to the anomaly observed along the east-west traverse. To investigate the sphere model and illustrate some of the non-uniqueness problems, the radius

and depth to centre of mass were calculated for an entire class of spherical bodies producing anomalies with a maximum peak of 5 mGal. The density contrast between these spherical bodies and the surrounding material ranged between 100 to 800 kg m^{-3}, allowing for a large class of geological materials (figure 8). The anomalies produced by these bodies of varying density, depth and radius were compared to the observed anomaly, and the body parameters producing anomalies which matched the data within the errors of the observations were found and are indicated in figure 8. For a spherical body, the centre of mass must be located at a depth of 1400±475 m, the density contrast must be greater than approximately 100 kg m^{-3} and the radius less than 1900 m.

5.2 $2\frac{1}{2}$ Dimensional Modelling :

Forward modelling of the gravity data was performed with the GSC interactive modelling program MAGRAV2 (Broome, 1989). This program is based on the two-dimensional modelling algorithm published by Talwani and Heirtzler (1964) with end corrections devised by Shuey and Pasquale (1973) (resulting in the so-called $2\frac{1}{2}$ dimensional modelling method).

The density, depth and size of the body causing the observed anomaly in the northern portion of the Dome are poorly constrained by geological information and not at all constrained by diamond drilling. Diamond drilling in the southern and western portions of the Dome structure indicated the presence of numerous dykes and sills of composition similar to the rhyolite porphyries outcropping over the Dome. A number of these drill holes intersected a porphyry body at depths ranging from 500 to 600 m. This body was not intersected in all the drill holes and was only penetrated to depths of 20 m; it is therefore possible that this body is only a sill. The lack of information about the northern portion of the Dome makes forward modelling difficult. Also, the possibility of multiple intrusions or an intrusion and denser alteration zone complicates the interpretation, since the observed anomaly may result from the combined effect of bodies having

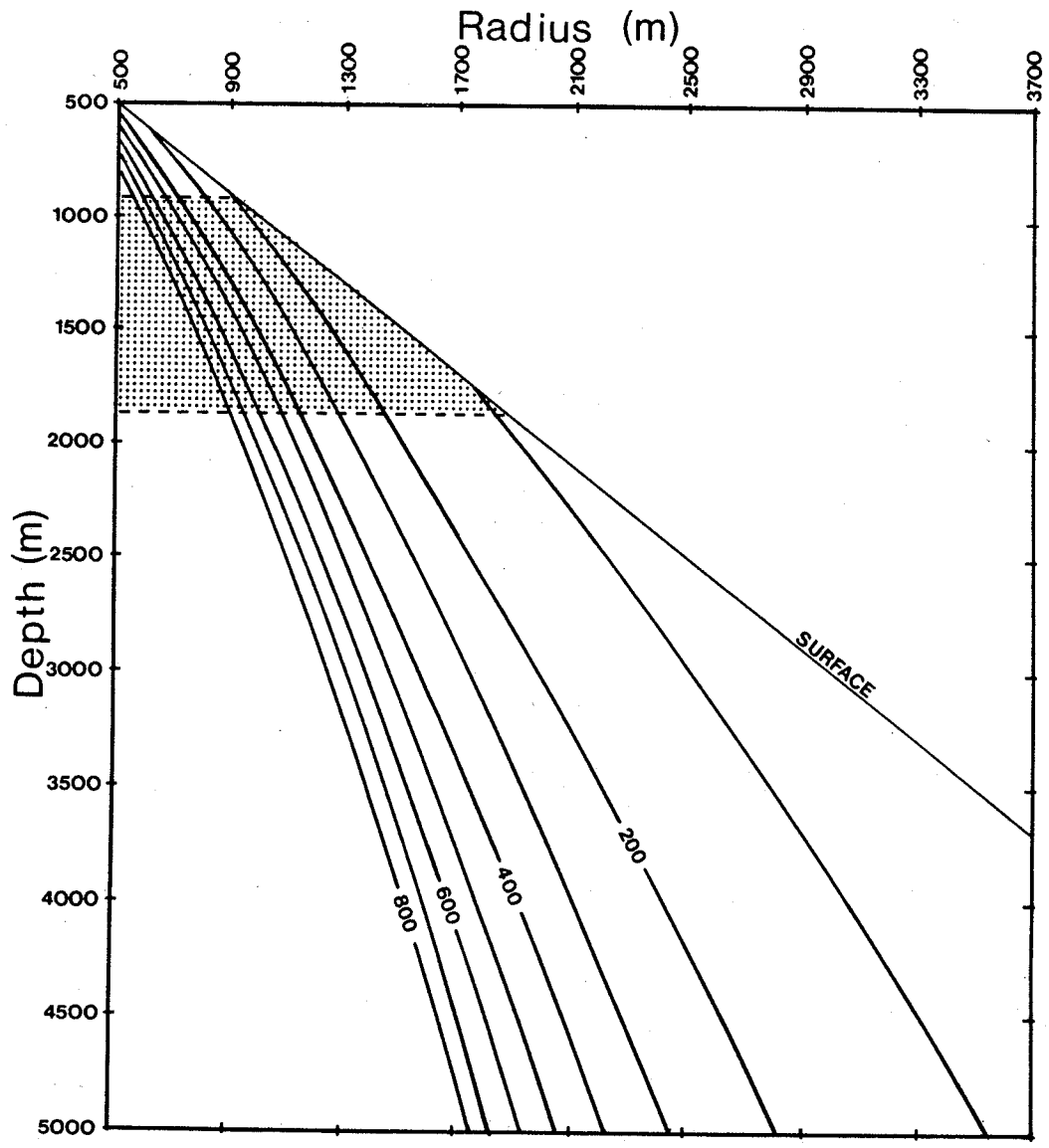

Figure 8 Plot of the parameters of spherical bodies producing 5 mGal peak anomalies for density contrasts from 100 to 800 kg m^{-3} in steps of 100 kg m^{-3}. Bodies within the stippled region have anomaly shapes fitting the observed anomaly. The vertical scale is depth to the centre of mass.

both positive and negative density contrasts.

Figure 9. shows one possible model where the observed anomaly is produced by a finite layer having a density of 3500 kg m^{-3}. This model does not necesarily represent a geologically plausible body but does indicate the approximate mass and distribution of material required to produce the observed anomaly.

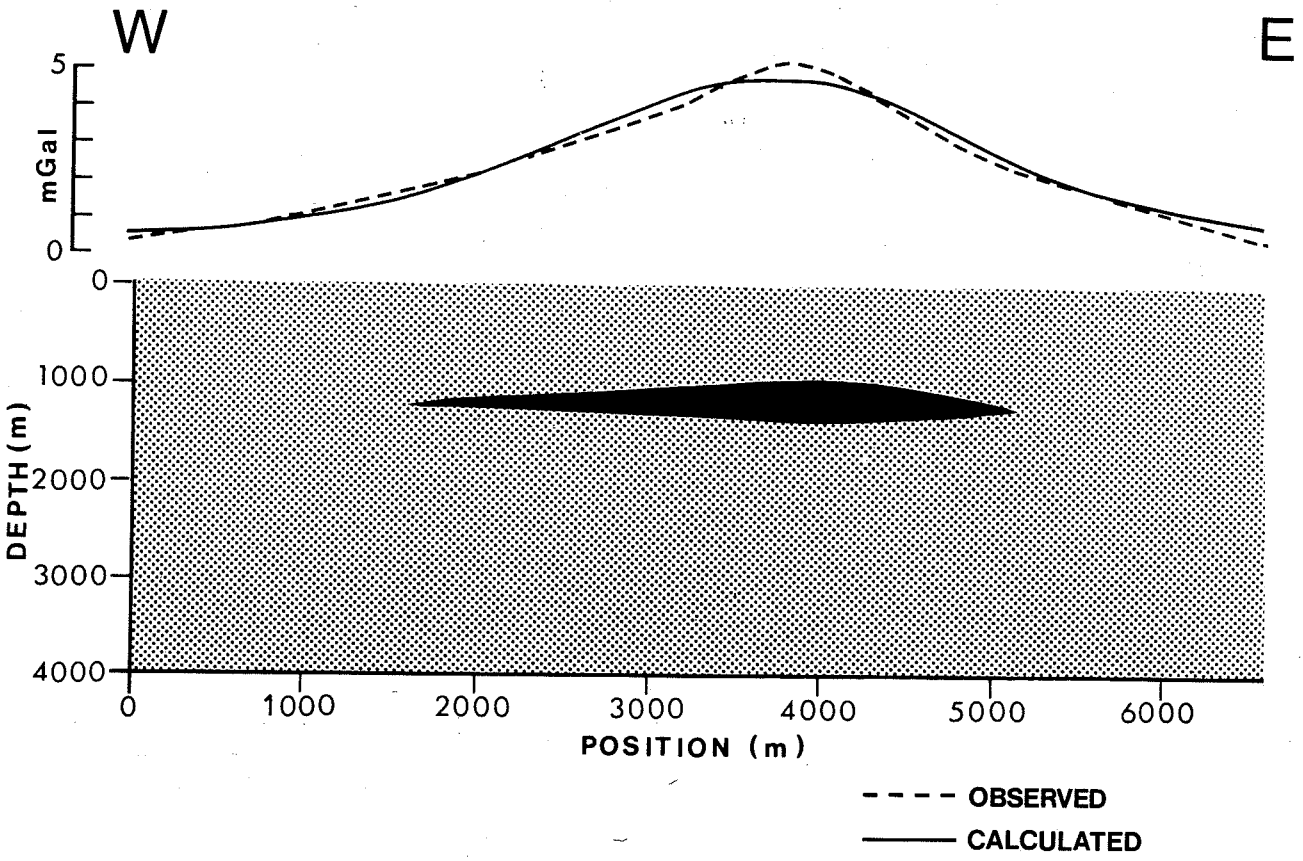

Figure 9 Model produced with MAGRAV2 showing a layer of density contrast 860 kg m^{-3} capable of producing the observed anomaly.

6
DISCUSSION AND CONCLUSIONS

Gravity observations from the Lemieux Dome indicate a north-south elongated positive Bouguer anomaly located over the northern portion of the dome structure. Interpretation of the observed anomaly suggests a value of 2.24×10^{12} kg for the excess mass of the body producing this anomaly. Approximating the anomalous body as a sphere with the centre of mass at a depth of 1400±475 m suggests a minimum density of 2730 kg m^{-3} is required to produce the observed anomaly (see figure 8).

Earlier geological and fluid inclusion studies indicated that the hydrothermal quartz-carbonate vein system and alteration of the sediments of the Dome required a heat source larger than indicated by the intrusives observed cutting the Dome. The fluids responsible for the mineralization of the quartz carbonate veins are interpreted to be at least partially magmatic in origin. The mineral zoning suggested that the heat source of the hydrothermal system was located in the northern portion of the Dome and related to the porphyritic intrusions (Stevens, 1986). The gravity survey however, indicated the presence of a positive anomaly in the proposed region of the heat source (figure 7). The rhyolite porphyry intrusives observed near the dome have densities of approximately 2600 ± 20 kg m^{-3} (Tanner and Uffen 1960; see also appendix C) and would produce a slightly negative response. Hence the anomalous body must be more dense than the porphyries observed in the region. The anomaly could be produced by a gabbroic intrusion, poly-phase felsic intrusion or a skarn zone related to an intrusion.

It is possible that the anomaly is the response of denser gabbroic intrusives, although these are thought to be related to the extrusive volcanics to the south of the Dome. Also, gabbroic intrusives have not been observed in large quantities in the region of the gravity anomaly. Models involving denser

phases related to the porphyritic intrusives can also be envisioned to explain the anomaly, but there is little evidence to support such assumptions.

One possible explanation for the anomalous body arises from drilling near the Mont Vallières de St. Réal intrusive, which is thought to have a similar geology to the Lemieux Dome. A thick (200 m) layer of andradite skarn was intersected and analysis of a core sample of the skarn provided by the Ministère de L'Energie et des Resources indicates that these rocks have a very high density of approximately 3490 kg m^{-3}. A similar skarn zone associated with the porphyritic intrusion on the Lemieux Dome may explain the observed gravity anomaly and the spatial correlation of the gravity anomaly with the porphyrytic intrusives and mineral zoning.

Density determinations from future drilling and geological surveys will place further constraints on the intrusive bodies of the Dome. If information on the depth, composition and/or density of the intrusive were available further forward modelling could be conducted.

Acknowledgements

Discussions with Gilles Duquette, the provincial resident geologist at Sainte-Anne-des-Monts, has contributed substantially to this work. The authors would like to thank the entire staff of the Resident Geologist's office for their hospitality and contributions to this work. The fluid inclusion and geological studies by K. Stevens (MSc, McGill, 1986) have helped tremendously in understanding the Dome and go a long way towards constraining plausible interpretations of the geophysical data. The authors would also like to thank Don Henderson, Dave Halliday and Warner Miles for assistance in acquisition and processing of the gravity data and Mike Thomas, Yvon Maurice and Ken Currie for carefully reading the manuscript and for helpful comments.

7
REFERENCES

1) Allcock, J.B., 1982. Skarn and porphyry copper mineralization at mines Gaspé, Murdochville, Québec. *Econ. Geol.*, **77**, pp. 971-999.

2) Bible, J.L., 1962. Terrain correction tables for gravity. *Geophysics*, **27**, pp. 715-718.

3) Broome, J., 1989. *MAGRAV2: An interactive magnetic and gravity modelling program for microcomputers (version 1.5).* Geol. Surv. Canada, Open File no.1334. 43 p.

4) de Römer, H.S., 1974. Geology and age of some plutons in north central Gaspé, Canada. *Canadian Jour. Earth Sci.*, **11**, pp. 570-582.

5) Doyon, M., Dalpé, C., and Valiquette, G., 1990. *Silurian and Devonian Volcanic Rocks of the Gaspé Peninsula.* Geol. Surv. Canada, Open file no.2235. pp. 67-71

6) Kearey, P., and Brooks, M., 1984. *An introduction to geophysical exploration.* Blackwell Scientific Publications, Palo Alto, California. 296 p.

7) La Rocque, C., 1986. *Geochronology and petrology of north-central Gaspé igneous rocks, Québec.* Unpub. M.Sc. thesis, McGill Univ.. 231 p.

8) Laurent, R., and Bélanger, J., 1984. Geochemistry of Silurian-Devonian alkaline basalt suites from the Gaspé Peninsula, Québec Appalachians. *Maritime Sediments and Atlantic Geology*, **20**, pp.67-78.

9) Lebel, D., and Hubert, C., 1986. Acadian wrench tectonics in the Rimouski-Matapedia area of the Québec Appalachians: a model. *Geological Asscoiation of Canada, Programs with Abstracts*, **11**, p.94.

10) Longman, I.M., 1959. Formulas for computing the tidal accelerations due to the moon and sun. *Jour. Geophysical Research*, **64**, 2351-2355.

11) Shuey, R.T., and Pasquale, A.S., 1973. End corrections in magnetic profile

interpretation. *Geophysics*, **38**, pp. 507-512.

12) Stevens, K., 1986. *Fluid inclusion and geological studies on the Zn-Pb-Cu vein system at Lemieux Dome, Gaspé, Québec.* Unpub. M.Sc. thesis, McGill Univ.. 150 p.

13) Talwani, M., and Heirtzler, J.R., 1963. *Computation of magnetic anomalies caused by two dimensional structures of arbitrary shape.* Computers in the Mineral Industry, School of Earth Sciences, Stanford University. pp. 465-480

14) Tanner, J.G., and Uffen, R.J., 1960. Gravity anomalies in the Gaspé Peninsula, Québec. *Dominion Observatory*, **21**, pp. 221-237.

15) Whalen, J., 1988. Granitic rocks of New Brunswick and Gaspé, Québec: a transect across the southern Canadian Appalachians. *Geological Asscoiation of Canada, Programs with Abstracts*, **13**, pp. 133-134.

16) Wilson, J.T., 1966. Did the Atlantic close and then re-open ?. *Nature*, **211**, pp. 676-681.

MAPS

1:20,000 Aeromagnetic total field (map 21075G), published by Geological Survey of Canada, 1985

1:20,000 Aeromagnetic vertical gradient (map 41075G), published by Geological Survey of Canada, 1985

1:50,000 Topographic (maps 22B/9 and 22B/16), published by Geological Survey of Canada

1:250,000 Topographic (maps 22A, 22B, 22G and 22H), published by Geological Survey of Canada

1:20,000 Geological (Lac Sainte-Anne 22B 16-200-0102), published by Ministère de l'Énergie et des Ressources, Québec

APPENDIX A Gravity Data

Station Number	Date	Time (GMT)	UTM Easting (m)	UTM Northing (m)	Zone	Elevation (m)	Tide Corr. (mGal)	Terrain Corr. (mGal)	Observed Gravity (mGal)	Free-air Anomaly (mGal)	Bouguer Anomaly (mGal)
7502	88/08/21	19:32	708095	5406905	19NW	365.8	-0.062	6.0	980870.457	22.85	-12.11
7503	88/08/21	18:57	708045	5406055	19NW	336.8	-0.054	6.4	980873.538	17.67	-13.61
7504	88/08/21	14:41	707815	5405660	19NW	341.1	-0.049	6.5	980875.181	20.95	-10.73
7505	88/08/21	18:30	707945	5405290	19NW	338.0	-0.046	5.5	980876.202	21.31	-11.00
7506	88/08/21	19:18	708025	5406520	19NW	362.4	-0.059	5.7	980871.191	22.84	-11.99
7507	88/08/22	14:23	708100	5406980	19NW	368.5	0.080	6.7	980870.314	23.48	-11.11
7508	88/08/22	14:39	707965	5407400	19NW	378.6	0.075	5.7	980868.497	24.44	-12.27
7509	88/08/22	14:50	707955	5407900	19NW	384.0	0.071	5.6	980868.504	25.71	-11.67
7510	88/08/22	14:59	707705	5408320	19NW	395.6	0.068	5.9	980867.625	28.06	-10.34
7511	88/08/22	15:09	707425	5408680	19NW	406.3	0.064	6.1	980866.770	30.22	-9.12
7512	88/08/22	15:17	707195	5409155	19NW	421.8	0.061	5.8	980865.952	33.79	-7.68
7513	88/08/22	15:31	706795	5409705	19NW	427.6	0.055	5.2	980867.255	36.42	-6.27
7514	88/08/22	15:40	706710	5410230	19NW	435.6	0.051	5.1	980866.640	37.85	-5.81
7515	88/08/22	15:48	706995	5410620	19NW	447.4	0.047	5.0	980865.297	39.84	-5.22
7516	88/08/22	16:04	707255	5411005	19NW	463.0	0.039	4.6	980863.391	42.45	-4.77
7517	88/08/22	16:36	707515	5411435	19NW	464.8	0.023	5.3	980860.359	39.63	-7.09
7518	88/08/22	16:46	707350	5411855	19NW	489.5	0.017	4.9	980859.374	45.93	-3.94
7519	88/08/22	16:57	707140	5412280	19NW	504.7	0.012	4.6	980857.755	48.65	-3.29
7520	88/08/22	17:07	707015	5412740	19NW	524.3	0.006	3.9	980855.904	52.47	-2.27
7521	88/08/22	17:18	707120	5413145	19NW	552.0	0.000	4.3	980852.575	57.37	0.13
7522	88/08/22	17:28	707185	5413600	19NW	595.9	-0.005	2.7	980847.052	65.03	1.04
7523	88/08/22	17:40	707790	5413730	19NW	652.6	-0.011	3.0	980836.295	71.68	1.67
7524	88/08/22	17:56	707970	5413980	19NW	650.7	-0.019	3.0	980837.881	72.49	2.70
7525	88/08/22	18:09	708355	5414595	19NW	643.4	-0.026	4.2	980833.402	65.27	-2.56
7526	88/08/22	18:18	708520	5415110	19NW	679.7	-0.030	3.8	980834.000	76.66	4.41
7527	88/08/22	18:28	709050	5415205	19NW	625.1	-0.035	3.7	980844.558	70.31	4.04

Station Number	Date	Time (GMT)	UTM Easting (m)	UTM Northing (m)	Zone	Elevation (m)	Tide Corr. (mGal)	Terrain Corr. (mGal)	Observed Gravity (mGal)	Free-air Anomaly (mGal)	Bouguer Anomaly (mGal)
7528	88/08/22	18:49	709647	5415190	19NW	579.4	-0.044	3.6	980851.967	63.64	2.36
7529	88/08/22	18:59	710145	5414895	19NW	562.7	-0.049	4.0	980855.045	61.82	2.81
7530	88/08/20	13:19	710375	5425505	19NW	201.2	0.031	8.7	980934.719	21.39	7.59
7531	88/08/20	13:53	710610	5424620	19NW	235.0	0.021	8.1	980930.250	28.07	9.84
7532	88/08/20	14:23	711470	5423685	19NW	260.0	0.013	7.1	980925.855	32.45	10.38
7533	88/08/20	14:53	711865	5422750	19NW	266.7	0.004	9.4	980925.956	35.11	14.65
7534	88/08/20	15:08	712345	5421880	19NW	276.8	0.000	14.7	980922.587	35.57	19.32
7535	88/08/20	15:20	712345	5421475	19NW	267.0	-0.004	13.3	980925.475	35.76	19.17
7536	88/08/20	15:35	712450	5420545	19NW	275.2	-0.008	12.3	980925.641	39.21	20.69
7537	88/08/20	15:47	712420	5419350	19NW	282.9	-0.011	11.7	980924.500	41.41	21.47
7538	88/08/20	16:03	711990	5418505	19NW	301.4	-0.015	6.6	980917.502	40.79	13.62
7539	88/08/20	16:15	711510	5417905	19NW	301.8	-0.018	5.3	980915.189	39.07	10.57
7540	88/08/20	16:50	712290	5417200	19NW	312.7	-0.027	5.7	980906.880	34.71	5.41
7541	88/08/20	17:27	712670	5415970	19NW	337.7	-0.035	6.5	980894.826	31.38	0.09
7542	88/08/20	17:44	713030	5414780	19NW	343.2	-0.039	6.4	980890.277	29.50	-2.54
7543	88/08/20	17:58	712970	5413545	19NW	358.1	-0.041	5.5	980886.741	31.55	-3.06
7544	88/08/20	18:14	713495	5412705	19NW	408.4	-0.044	3.5	980876.536	37.56	-4.64
7545	88/08/20	18:35	713980	5412105	19NW	428.9	-0.048	3.4	980871.207	39.06	-5.54
7546	88/08/20	18:48	713770	5411145	19NW	444.7	-0.050	3.4	980868.494	41.99	-4.35
7547	88/08/20	19:02	712750	5410615	19NW	452.3	-0.052	3.5	980864.980	41.22	-5.96
7548	88/08/20	19:15	712345	5409730	19NW	498.7	-0.054	3.2	980854.628	45.89	-6.74
7549	88/08/20	19:43	712095	5408650	19NW	574.2	-0.058	2.8	980838.4108	53.83	-7.60
7550	88/08/20	19:53	711560	5407795	19NW	538.6	-0.059	2.9	980843.664	48.77	-8.64
7551	88/08/20	20:04	711040	5407195	19NW	496.8	-0.060	2.7	980850.322	43.00	-9.93
7552	88/08/20	20:16	710530	5406360	19NW	427.6	-0.062	3.6	980860.978	32.96	-11.29
7553	88/08/20	20:30	710180	5405460	19NW	402.9	-0.064	4.2	980865.008	30.08	-10.86

Station Number	Date	Time (GMT)	UTM Easting (m)	UTM Northing (m)	Zone	Elevation (m)	Tide Corr. (mGal)	Terrain Corr. (mGal)	Observed Gravity (mGal)	Free-air Anomaly (mGal)	Bouguer Anomaly (mGal)
7554	88/08/20	20:40	710480	5404505	19NW	391.4	-0.065	3.6	980866.802	29.10	-11.09
7555	88/08/20	20:54	710210	5403160	19NW	359.4	-0.066	3.6	980872.373	25.88	-10.74
7556	88/08/20	21:15	710345	5402225	19NW	327.1	-0.069	3.5	980877.986	22.28	-10.84
7557	88/08/21	13:25	709950	5400780	19NW	296.6	0.063	2.9	980882.142	18.18	-12.15
7558	88/08/21	13:41	709370	5399540	19NW	280.1	0.059	2.4	980883.390	15.32	-13.62
7559	88/08/21	13:55	709050	5398560	19NW	254.8	0.055	2.7	980886.516	11.42	-14.37
7560	88/08/21	14:08	708905	5397655	19NW	236.8	0.051	4.1	980888.968	9.04	-13.37
7561	88/08/21	14:16	709275	5396720	19NW	224.6	0.049	3.7	980889.681	6.75	-14.69
7562	88/08/21	14:37	709495	5395755	19NW	219.8	0.041	3.8	980888.972	5.35	-15.46
7563	88/08/21	14:50	710405	5394525	19NW	202.1	0.037	4.1	980890.093	2.03	-16.47
7564	88/08/21	15:03	710175	5393740	19NW	175.6	0.032	4.3	980892.944	-2.67	-18.04
7565	88/08/21	15:13	709005	5392470	19NW	150.6	0.028	7.3	980895.112	-7.23	-16.81
7566	88/08/24	13:45	709870	5406290	19NW	533.4	0.117	2.8	980841.606	46.27	-10.68
7567	88/08/24	14:00	710050	5406590	19NW	570.9	0.120	5.2	980835.101	51.10	-7.61
7568	88/08/24	14:11	709800	5406940	19NW	579.7	0.121	4.0	980833.489	51.92	-9.01
7569	88/08/24	14:20	709655	5407230	19NW	591.9	0.121	4.3	980831.835	53.79	-8.12
7570	88/08/24	14:29	710040	5407435	19NW	623.9	0.122	5.9	980826.002	57.68	-6.26
7571	88/08/24	14:44	709785	5407645	19NW	656.5	0.121	7.0	980820.042	61.60	-4.92
7572	88/08/24	14:55	709655	5408110	19NW	673.9	0.120	6.8	980817.490	64.04	-4.58
7573	88/08/24	15:06	709470	5408610	19NW	690.4	0.118	6.0	980814.725	65.96	-5.31
7574	88/08/24	15:17	709255	5409180	19NW	701.6	0.116	5.8	980813.058	67.28	-5.49
7575	88/08/24	15:26	709250	5409660	19NW	712.3	0.114	6.1	980812.456	69.59	-4.09
7576	88/08/24	15:37	709340	5410125	19NW	693.4	0.110	7.1	980815.747	66.68	-3.83
7577	88/08/24	15:51	709425	5410700	19NW	725.7	0.105	7.1	980812.115	72.55	-1.58
7578	88/08/24	16:10	708960	5410780	19NW	777.8	0.097	7.0	980801.031	77.47	-2.63
7579	88/08/24	16:35	708620	5411005	19NW	720.9	0.085	6.1	980812.661	71.35	-3.24

Station Number	Date	Time (GMT)	UTM Easting (m)	UTM Northing (m)	Zone	Elevation (m)	Tide Corr. (mGal)	Terrain Corr. (mGal)	Observed Gravity (mGal)	Free-air Anomaly (mGal)	Bouguer Anomaly (mGal)
7580	88/08/24	17:28	709880	5410755	19NW	796.7	0.052	8.1	980797.517	79.84	-1.26
7581	88/08/24	17:49	710200	5411160	19NW	798.9	0.037	7.8	980796.672	79.35	-2.29
7582	88/08/24	18:04	710635	5410925	19NW	824.5	0.026	10.1	980791.493	82.28	0.09
7583	88/08/24	18:19	711140	5410840	19NW	764.1	0.015	8.5	980803.515	75.74	-1.30
7584	88/08/24	18:36	711445	5410445	19NW	727.9	0.003	6.7	980811.641	73.02	-1.72

APPENDIX B Air Density and Barometric Pressure Correction

Correction for variation of air density :

The following equation was used to perform the corrections for variations in the temperature and moisture content of the air (Field procedures manual, Geological Survey of Canada, Geophysics Division unpublished manuscript, 1986). The reading at the first base was taken as a reference value and all other readings in the traverse were corrected relative to this reading.

$$A_1 = R_1 = \quad \text{uncorrected altimeter reading at known \#1}$$

$$A_i = (R_i - R_{i-1}) \cdot [\frac{1 + 0.00204 \cdot (D_i - 50)}{1 - 0.378 \cdot (10^{EXP}/29.9)}] + A_{i-1} \quad i = 2, ...N$$

where EXP $= -0.744112 + 0.01835 \cdot (W_i - 32)$.

R_i = altimeter reading

A_i = altimeter reading at station "i" corrected for humidity and temperature

D_i = dry bulb temperature (°F) at station "i"

W_i = wet bulb temperature (°F) at station "i"

Correction for barometric pressure drift :

Altimeter readings were corrected for drift by assuming that the drift was a linear function of time. The equation used for this correction was:

$$E_i = A_i - \frac{t_i - T_1}{T_2 - T_1} \cdot [(A_2 - A_1) - (K_2 - K_1)]$$

where E_i = final computed elevation for station "i"

A_i = altimeter reading corrected for density

t_i = time of altimeter observation at station "i"

T_1, T_2 = times of observations of known #1 and known #2

K_1, K_2 = known elevations of known #1 and known #2.

Note: measurements are recorded and processed in feet and Fahrenheit degrees, the final elevation is then converted to metric units.

APPENDIX C Hand Samples

Sample No.	Density
WXMG32	2606 kg m^{-3}
WXMG76	2594 kg m^{-3}
WXMG77	2636 kg m^{-3}
WXMG80	2581 kg m^{-3}
WXMG82	2583 kg m^{-3}
WXMG100	2585 kg m^{-3}
WXMG101	2683 kg m^{-3}

Samples collected by J. B. Whalen, from Hog's Back, Mont Chauve, and Mont Vallières de St. Réal believed to be representative of the phorphyry intrusives cutting the Lemieux Dome.